Effect of titanium and zirconium carbide interphases on the thermal conductivity and interfacial heat transfers in copper/diamond composite materials

Clio Azina, Iñaki Cornu, Jean-François Silvain, Yongfeng Lu, Jean-Luc Battaglia

Effect of titanium and zirconium carbide interphases on the thermal conductivity and interfacial heat transfers in copper/diamond composite materials

Clio AZINA,[a,b,‡,*] Iñaki CORNU,[a] Jean-François SILVAIN,[a,b] Yongfeng LU,[b] Jean-Luc BATTAGLIA [c]

[a] CNRS, University of Bordeaux, ICMCB, UMR 5026, F-33600, Pessac, France

[b] Department of Electrical and Computer Engineering, University of Nebraska-Lincoln, Lincoln, NE 68588-0511, United States

[c] CNRS, University of Bordeaux, I2M, UMR 5295, F-33400, Talence, France

Abstract

Thermal properties of metal matrix composite materials are becoming ever more relevant with the increasing demand for thermally efficient materials. In this work, the thermal conductivity and heat transfers at the interfaces of copper matrix composite materials reinforced with diamond particles (Cu/D) are discussed. The composite materials contain either ZrC or TiC interphases and exhibit, respectively, higher and lower thermal conductivities with respect to their pure Cu/D counterparts. These thermal conductivities are accounted to the presence of strong covalent bonds and increased relative densities. The role of these interphases is also discussed regarding the phonon transmission at the interfaces.

Keywords: metal-matrix composites (MMCs), interface/interphase, thermal properties, transport phenomena analysis

1. Introduction

Thermally efficient materials are constantly being studied for several engineering purposes such as heat-sinks in microelectronic components. Such materials allow proper heat dissipation and ensure a longer lifespan of the microelectronic assembly. In a constant effort to find highly conductive materials, numerous results have been reported regarding the copper(Cu)/diamond(D) system [1–3], and related interphases [4–13]. Indeed, composite materials, such as Cu/D, are attractive because of their ability to combine the properties of both

‡ Present address: Thin Film Physics Division, Department of Physics, Chemistry and Biology (IFM), Linköping University, SE-58183 Linköping, Sweden

constituting phases. However, in the absence of an appropriate interface between Cu and D, the thermal conductance h_c at the interface is low, resulting in a lower effective thermal conductivity, K_{eff}, with respect to the conductivity of pure Cu.

Several values of K_{eff} have been reported in the literature for the Cu/D system that vary according to the fabrication process, as well as to the properties of the reinforcement in terms of volume fraction f_d, characteristic dimension d, shape, and thermal conductivity k_d. Indeed, for a composite without interfacial layers, Schubert et *al*. reported K_{eff} = 215 $W.m^{-1}.K^{-1}$ for f_d = 42 % and d = 120 μm [1]. On the other hand, Tao et *al*. reported that K_{eff} varied from 150 down to 42 $W.m^{-1}.K^{-1}$ when f_d varied respectively from 50 to 70 % for d = 40 μm [3]. More recently, He et *al*. reported a value of K_{eff} = 414 $Wm^{-1}K^{-1}$ for f_d = 90 % and d = 220-245 μm, meaning that a slightly higher value of the equivalent thermal conductivity than that of copper can be reached without the presence of an interfacial layer [9]. Yoshida and Morigami reported the highest thermal conductivity for a pure Cu/D system as K_{eff} = 742 $W.m^{-1}.K^{-1}$ for f_d = 70 % and d = 90 -100 μm, the thermal conductance of the interface being about $h_c \approx 3\times10^7$ $W.m^{-2}.K^{-1}$ [2]. Their remarkable result comes from the elevated sintering temperature and pressure of T_s = 1180 °C and P_s = 4.5 GPa, respectively, during 15 min using a belt-type high-pressure apparatus [14]. However, performing sintering at very high temperatures and pressures during short durations is not available at the industrial level, although progress is continuously reported.

All these results showed that despite the weak interfacial bonding between Cu and D, an increase of the composite's thermal conductivity is expected when increasing the size of the diamond particles and performing fastest hot-pressing processes. Obviously, the dependence of the thermal conductivity on the diamond particle size indicates that the interfacial thermal barrier must be considered. However, it has also been shown that the increase in the thermal conductance at the interface between metals and diamond is still weak, and that it tends to saturate at very high pressures [15]. In a non-reactive system such as Cu-D, the creation of an interphase, for example a carbide layer or submicronic Cu particles attached through oxygen bonds to the matrix and reinforcements [16], will allow a better transfer of thermal and thermo-mechanical load from one phase to the other. In this work we focus on the insertion of carbide interphases.

As reported by Schmidt-Brüken et *al*. [5] and Dewar et *al*. [6], alloying of copper with a strong carbide forming element promotes wetting and bonding with diamond and leads to a significant increase of the thermal conductivity. It has been well established that the thermal

conductivity is higher as the chemical bond between matrix and reinforcement is stronger [17]. Bond strength enhancement has been observed with addition of Ti, Cr, Zr, and B in the Cu powder prior to the sintering process. Two main physical phenomena can explain the increase in thermal conductivity. The first one is related to the chemical bond between the carbide layer and both the diamond and Cu, and the second one is related to the role of the interphase regarding the heat transfer process at the nanoscale between two very different materials [15]. Indeed, electrons are responsible for the heat transfer in copper whereas phonons dominate in diamond. Regarding the Cu-D system, the electron-phonon coupling model is insufficient to explain the conductance at the metal-dielectric interface. Due to the low cut-off frequency of phonons in metals and the very high one for diamond, only inelastic processes, such as the three-phonon scattering process, are able to explain the measured interfacial extra conductance beyond the radiation limit, resulting from the elastic two-phonon process. The necessary coupling between phonons is then largely improved by inserting an interphase between the two materials. However, this layer must be chosen carefully in terms of its intrinsic thermal conductivity, Debye temperature and thickness. As revealed by Weber and Tavangar, the concentration of the active element, forming the carbide interphase, must not exceed the limit required for carbide formation [10].

We report in **Table 1** several thermal conductivities obtained from the literature which consider different carbide interphases, and different sintering parameters. Although some inconsistencies occur, remarkable trends can easily be identified to reach the highest thermal conductivity of the composite material. Some conditions which stand out are: (i) high heating rates dT/dt (°C.min^{-1}), (ii) reinforcement contents which are close or exceed the percolation threshold, (iii) large reinforcement sizes (d > 120 μm), and (iv) interphase thicknesses, e_X, that are higher than the mean free path of hot carriers. Condition (iv) allows maximizing the elastic scattering of phonons at the interface between the interphase and both adjacent materials (the matrix and the particle). The results obtained by Li et *al*. [12,18] that reported a thermal conductivity exceeding 900 W.m^{-1}.K^{-1} for a CuZr0.5 composite with d = 230 μm, and f_d = 0.61, and a thermal conductivity exceeding 750 W.m^{-1}.K^{-1} for a CuTi0.5 with same values for d and f_d, should be pointed out. The authors attribute these extremely high values of TCs to the optimized ZrC and TiC interphases formed using the gas pressure infiltration method. Therefore, the upper limit for e_X must be chosen in order to respect condition (iv) but also to lead to the best bonding at both the diamond/carbide and carbide-copper interfaces. However, the choice of the active element remains questionable regarding the values reported in **Table**

1 where similar values for K_{eff} are found using either Cr, Ti, Zr or W with optimal values of d, f_d and sintering parameters. In addition, it is not clear that diamond particles coated with the active element would lead to significant improvement with respect to uncoated particles.

Table 1: Measured effective thermal conductivities K_{eff} of the Cu/X/Diamond composites, X being the carbide interphases (B_4C, Cr_3C_2, TiC, ZrC, WC), and h_c. IHP: indirectly heated hot pressing, DHP: directly heated hot pressing, SPS: spark plasma sintering, PPS: pulse plasma sintering, GPI: gas pressure infiltration route.

	D (µm)	f_d	e_x (nm) / h_c[a] ($MW.m^{-2}.K^{-1}$)	K_{eff} ($W.m^{-1}.K^{-1}$)	T_s (°C)/ P_s (GPa)/ dT/dt (°C/min) (heating duration, process)
CuCr0.8 [4]	120	0.42	-/17	482	950/-/- (1h, IHP)
	120	0.42	-/94	639	950/-/- (30 min, DHP)
CuCr0.8 [1]	177-210	0.5	-/50	640	-/-/-
CuCr[d 7]	70	0.65[b]	1000/34	562	1150/0.02/- (10 min)
CuCr[d8]	100	0.5	1000/-	284	920/0.03/110 (SPS)
CuCr[d19]	200	0.5	200/21	589	900/0.08/- (10 min, PPS)
CuB0.3[4]	120	0.42		490	950/-/- (1h)
CuTi1[4]	120	0.42		290	950/-/- (1h)
CuTi0.6[11]	300	0.5	272/-	620	1646/0.7/- (30 min)[c]
CuTi0.5[e20]	180	0.5	-/48	630	1000/0.05/50 (10 min, SPS)
CuTi0.5[18]	230	0.61[b]	200 -300/-	752	1150/0.01/- (10 min, GPI)
CuZr1[9]	220 - 245	0.9[b]	-/5.9[b]	677	1500/5/- (10 min)[c]
CuZr0.7[4]	120	0.42		285	950/-/- (1h)

CuZr0.5[12]	230	0.61[b]	300/75	930	1150/0.01/- (10 min, GPI)
CuW5[f21]	200 - 300	0.46	200/-	672	927/-/- (6 min, SPS)
CuW[g22]	160 - 250	0.48	260/45	690	900/0.08/- (10 min, PPS)

[a] The thermal conductance of the interphase, h_c, is calculated using the Hasselman and Johnson model [23]. [b] percolation is reached, making the Hasselman and Johnson model non-applicable; [c] liquid Cu phase sintering; [d] Cr-coated diamond, e_X indicates the coating thickness; [e] Ti-coated diamond, e_X indicates the coating thickness; [f] pretreatment of diamond particles at 1313 K; [g] W-coated diamond, e_X indicates the coating thickness.

The experimental data are well predicted, according to the authors of the mentioned works, from the theoretical models of the effective thermal conductivity derived, for instance, by Hasselman and Johnson [23] (H-J model). These models show that increasing the volume fraction of D in the Cu matrix, when h_c does not reach the minimal value at a given value of particle diameter, d, leads to a significant decrease of the effective thermal conductivity of the composite. The H-J model rests on the Maxwell approach that assumes the dilution of the diamond particles within the matrix. Indeed, in the derivation by Maxwell, the assumption has been made that the average distance between the particles of the discontinuous phase is large enough so that the fields around individual particles are undisturbed by the presence of the other particles. However, as reported in the work of S. Whitaker, based on the volume averaging method [24], the analytical model of Maxwell is retrieved by considering a unit cell as that described by Chang [25,26]. This configuration assumes a periodic arrangement of the unit cells and a temperature gradient for two parallel faces of the cube whereas the other perpendicular faces to the temperature gradient are insulated.

In the present paper we report the Cu(Cu-Ti)/D and Cu(Cu-Zr)/D systems obtained through the solid-liquid coexistent phase process [27], and their corresponding thermal conductivities, as well as the heat transfers at the interphases before and after the percolation threshold. We discuss the role of the carbide interphase in the elastic and inelastic phonon-phonon processes and the contribution of chemical bonding at the involved interfaces within the measured enhancement of interfacial thermal conductance between copper and diamond. Theoretical

values of K_{eff} are calculated using both the H-J model and finite element ~~obtained based on~~ simulations of the heat transfer within the representative elementary volume of the composite considering randomly distributed particles. Both approaches are investigated. The average thermal resistance $R_c = 1/h_c$, at the particle-matrix interface, is then identified by comparing the experimental values and the theoretical ones for each type of interphase. Finally, these values of R_c are compared to the theoretical expectations calculated using the Diffuse Mismatch Model (DMM).

2. Materials and methods

2.1.Interphase creation

The copper-based matrix is composed of a mixture of dendritic copper powder (Eckart Granulate Velden GmbH) (d_{50} close to 35 μm) and either Cu-Ti alloyed powder with a composition of 21.79 wt.% in Ti (d_{50} close to 15 μm) or Cu-Zr alloyed powder with a composition of 8.6 wt.% in Zr (d_{50} close to 9 μm), both produced by atomization and supplied by Nanoval GmbH. The Cu-Ti content was varied between 2 and 6 vol.% and Cu-Zr was maintained at 14 vol.%, with respect to the total composite volume. The volume fractions used correspond to those which have resulted in the highest thermal conductivities in preliminary investigations. Grade MBD6 diamond particles of d_{50} ranging from 40 to 220 μm (Henan Zhongxing Corporation), were used as reinforcements (k_d = 1000-1500 $W.m^{-1}.K^{-1}$ thermal conductivity). The copper powders and reinforcements are mixed together using a 3D mixing device during 90 min at 20 RPM. Composite materials reinforced with diamond particles were sintered using a TermolabTM press. The powders were pre-compacted in a graphite mold before sintering. The pure Cu/D composites were sintered at 650 °C under 40 MPa of pressure for 30 min, the powders containing Ti were hot-pressed at 950 ºC under 40 MPa for 30 min, while those containing Zr were hot-pressed at 1050 °C under 40 MPa for 45 min. No squeezing of the liquid was observed during the sintering process, which we explain by the very small amount of liquid generated. The heating is ensured using an induction system, while the pressure is applied through the means of a hydraulic press. The temperature is controlled with the use of a thermocouple (type K) which is inserted into the mould. The chamber is put under vacuum (10^{-2} mbar range) to prevent the oxidation of the copper matrix during heating and/or cooling.

In the following sections we will be referring to the composite materials using the following nomenclature: Cu(Cu-*X*)*y*/D*z*, where *X* is either Ti or Zr, *y* is the volume percentage of Cu-X alloy with respect to the total volume, and *z* is the volume percentage of diamond particles.

2.2.Characterization

Cryofractures were carried out in liquid nitrogen. The microstructures of each composite were analyzed using scanning electron microscopy (SEM) (TESCAN VEGA 2 SBH) in secondary and back-scattered electrons mode, to deduce chemical information through apparent chemical contrast.

X-ray diffraction patterns were collected on a PANalytical X'pert PRO MPD diffractometer. The patterns were analyzed using EVA software (Bruker).

Due to the difficulty of machining diamond-based materials, preliminary studies were carried out on carbon fiber reinforced composite materials [27]. For the purpose of this article, the interphase thicknesses were considered to be the same for both carbon fiber and diamond particle-reinforced composites.

2.3.Thermal measurements

The thermal diffusivity of the composite materials was measured using a specific photothermal technique based on a periodic pulse (duration of 20 ns) waveform of the photothermal source[29]. This technique has been developed to deal with highly conductive materials without the need of absorbing/emitting coatings on both faces of the sample. The standard deviation of the measurement is less than 2 %. The average specific heat for each sample is calculated using the volume-based rule of mixture based on the densities and specific heats of Cu and diamond as well as on the volume fraction of diamond particles. The effective thermal conductivity is thereby calculated from the measured thermal diffusivity and the average specific heat.

3. Results and discussion

3.1. Experimental thermal conductivities

Figure 1 gathers the SEM micrographs obtained after cryofracture of the Cu/D40, Cu(Cu-Ti)4/D40, and Cu(Cu-Zr)14/D40 composite materials. One can observe the lack of cohesion at the interface between the Cu matrix and the diamond reinforcements in the case of the Cu/D40 composite material. This is due to the lack of chemical affinity between the constituents. The shock induced by the cryofracture caused a certain amount of diamond particles to detach from the matrix, leaving traces of their initial positions. The few diamond particles, which remained attached, are surrounded by voids which can clearly be seen in **Figure 1(a)**. However, the composite materials synthesized with either Cu-Ti or Cu-Zr

exhibit a completely different behavior when under harsh mechanical solicitation, such as cryofracture. Indeed, one can observe that instead of detaching, the diamond particles break and remain attached to the matrix. The high magnification micrographs given in **Figure 1(b)** and **(c)** show that the diamonds were split along particular planes, which indicates that the rupture was fragile.

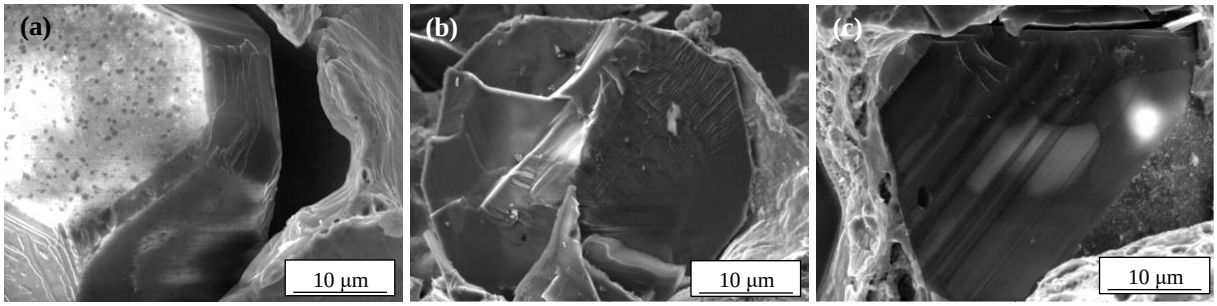

Figure 1: SEM micrographs of fractured surfaces of (a) Cu/D40, (b) Cu(Cu-Ti)4/D40, and (c) Cu(Cu-Zr)14/D40 composite materials after cryofracture in liquid nitrogen.

The measured thermal conductivity values reported in **Figure 2** correspond to those of the Cu/D and Cu(Cu-Ti)/D composite materials. As expected, the effective thermal conductivity of the Cu/D (gray spheres, **Figure 2**) composite material, without interphase, never exceeds that of copper (390 $W.m^{-1}.K^{-1}$) and tends to decrease with increasing f_d (> 0.3). This result is not surprising since the thermal contact at the diamond-copper interface is very low due to the purely mechanical bonds and very different phonon properties, as revealed by the Debye temperature of the two materials. The effective thermal conductivity of Cu(Cu-Ti)/D with particle diameter equal to 60 μm is higher, although it remains very comparable to the thermal conductivity of copper, when f_d = 0.4 (purple spheres, **Figure 2**). This disappointing result is explained by the fact that some Ti remains within the copper matrix and drastically decreases the thermal conductivity of the matrix and therefore that of K_{eff} [27].

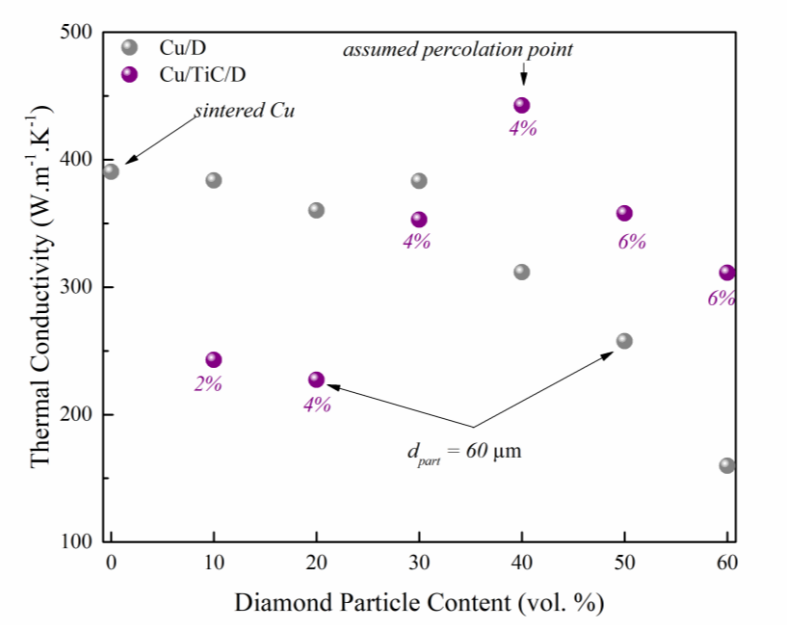

Figure 2: Thermal conductivities with respect to the diamond reinforcement content of the Cu/D (gray spheres) and Cu(Cu-Ti)/D (purple spheres) composite materials. The initial volume fraction of Cu-Ti in the composites are reported for each Cu(Cu-Ti)/D sample.

The XRD patterns presented in **Figure 3 (a)** and **(b)** show the contributions of TiC and ZrC respectively within the composite materials. While the presence of impurities within the Cu matrix is not necessarily detrimental to the properties, Ti has been shown to significantly decrease the electrical conductivity of pure Cu[31]. Therefore, one can expect that a small amount of Ti impurities within the composite could decrease the overall conductivity of the composite. To confirm this hypothesis a CuTi alloy (1 vol.% of Cu-Ti in Cu) has been synthesized. The value of the thermal conductivity of this alloy was deduced from the thermal diffusivity and is equal to 211 W.m^{-1}.K^{-1}. Here we show that the presence of Ti impurities can decrease the thermal conductivity of pure copper by almost half. Furthermore, SEM analyses on the alloy after chemical etching, revealed that the grain size of Cu corresponds to the initial dendrite sizes (**Figure 3 (c)**). When compared with an equivalent CuZr alloy ($k_{Cu\text{-}Zr}$ = 343 W.m^{-1}.K^{-1}), the grain size of the CuTi alloy is smaller.

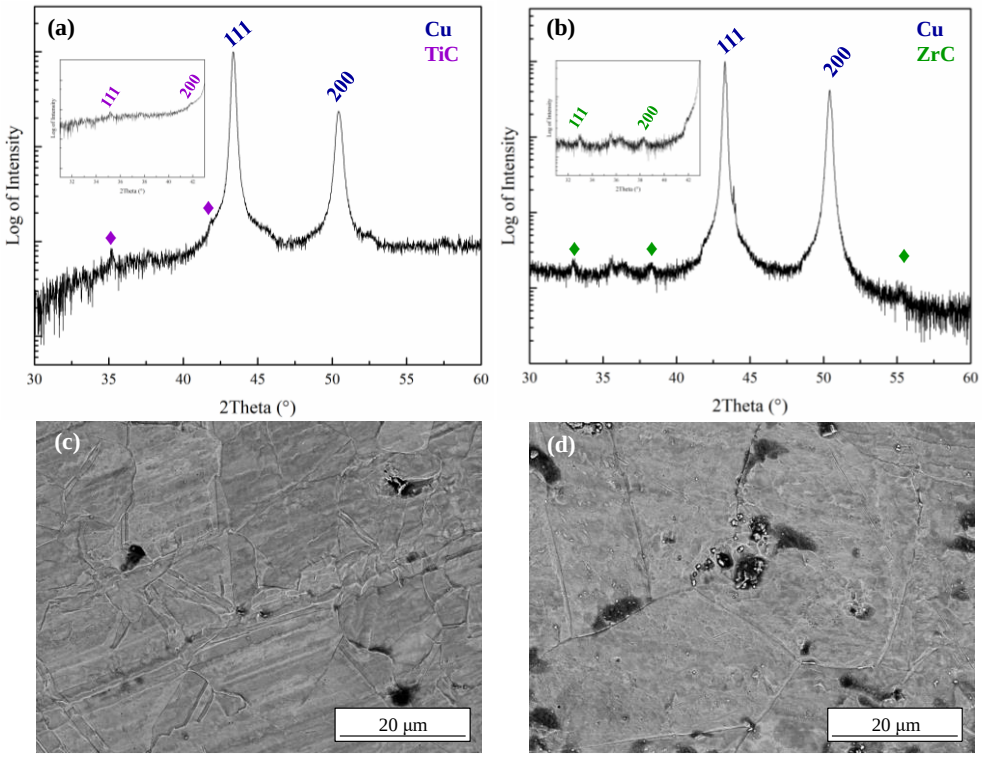

Figure 3: XRD patterns of (a) Cu(Cu-Ti)/D and (b) Cu(Cu-Zr)/D composite materials. (c) and (d) are SEM micrographs of chemically etched CuTi and CuZr alloys respectively.

Assuming the maximum of K_{eff} is reached close to the percolation limit, we measured the thermal conductivity of Cu(Cu-Zr)/D composites with f_d = 40 vol.% and we considered several values of particle diameter *d*, as shown in **Figure 4**. Results are more encouraging than those obtained with the TiC interphases even with the smallest diameter. The highest thermal conductivity K_{eff} = 584 $W.m^{-1}.K^{-1}$ was obtained with particles of 220 µm in diameter.

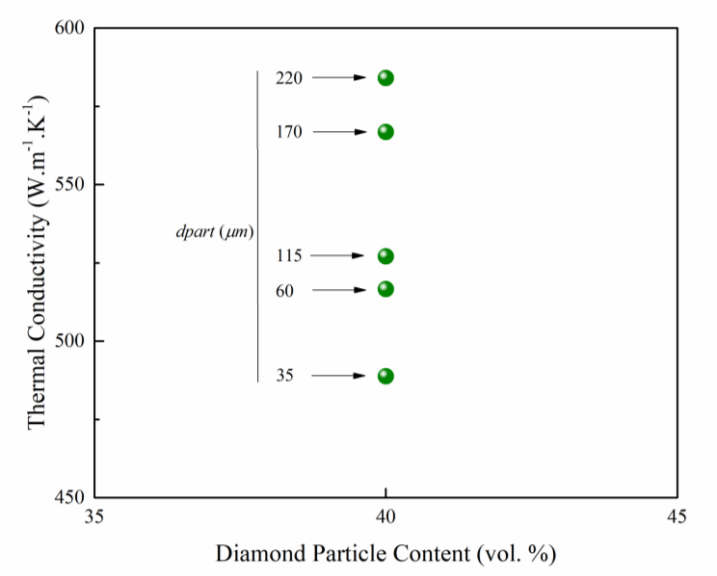

Figure 4: Thermal conductivities of Cu(Cu-Zr)/D composites with f_d = 40 vol.% for different particle sizes (d_{part}).

3.2.Analytical vs numerical models

The classical model of the effective thermal conductivity derived by Hasselman and Johnson (H-J, Equation 1) is valid when the volume fraction f_d is less than the value at percolation $f_{d,per}$ = 0.52 considering the particles of diameter d [23]. It must be noted however that the percolation threshold for randomly packed spheres is about 0.31 whereas the threshold for randomly packed diamond is expected to be around 0.42 (because of the faceted shape of the particles).

$$K_{eff} = k_m \frac{\left(\frac{k_d}{k_m} - \frac{k_d}{ah_c} - 1\right)f + \frac{k_d}{k_m} + \frac{2k_d}{ah_c} + 2}{\left(1 - \frac{k_d}{k_m} + \frac{k_d}{ah_c}\right)f + \frac{k_d}{k_m} + \frac{2k_d}{k_m} + 2} \quad (1)$$

As presented in **Figure 5(a)**, the dispersion process of diamond particles within the copper powder is not uniformly distributed. Therefore, we calculated also the effective thermal conductivity using the finite element (FE) method applied to a simulated medium, that is a cube with side a in which the spheres are randomly distributed, as presented in **Figure 5(b)**. The face of the simulation box is at a temperature of 0 K whereas the parallel face is at 1 K. All the other faces are insulated. The calculation of the effective thermal conductivity has been made considering, for a given value of f_d, three different random distributions of the particle. Therefore, it was verified that the calculated value does not change more than 2% between each simulation. In addition, the side a of the simulation box is chosen to be large enough in order to avoid fluctuations of the calculated values when changing the particle diameter. We found that using $a = 20 \times d$ allows to fulfil this requirement. The effective thermal conductivity K_{eff} is

calculated according to f_d and R_c for d = 60 µm and reported in **Figure 5(c)**. K_{eff} is also calculated according to R_c and d for f_d = 0.42 and reported in **Figure 5(d)**. The H-J model and the FE lead to comparable results. A small discrepancy occurs for large values of d and small values of R_c. These results lead to conclude about the non-significant influence of the particles distribution within the matrix when $f_d < f_{d,per}$. As shown, the effective thermal conductivity is slightly sensitive to the particles distribution when the resistance of the interphase is very low (see the results for $R_c = 4\times10^{-9}$ m^2.K.W^{-1}, for instance). However, such low values cannot be reached in practice since it is already lower than the intrinsic thermal conductivity e_i/k_i of the interphase without considering the resistances at both the Cu-interphase and interphase-diamond interfaces. On the other hand, **Figure 5(c)** shows that K_{eff} is equal or lower than that of copper when $R_c \geq 5.5 \times 10^{-8}\ m^2.K.W^{-1}$ whatever the volume fraction f_d. At this threshold value of R_c, the effective thermal conductivity K_{eff} is equal to that of copper k_m. In that case, relation (1) becomes $k_d = k_m/(1 - k_m/ah_c)$. As shown in **Figure 5(d)** this critical value increases significantly as the particle diameter increases. Finally, the uncertainty on the value of the thermal conductivity of the diamond particles must be considered since both materials constitutive of the composite are very conductive. Since measuring an accurate value on small grains is a very challenging task, the identification of both R_c and k_d, starting from experimental values of K_{eff}, is carried out and discussed later.

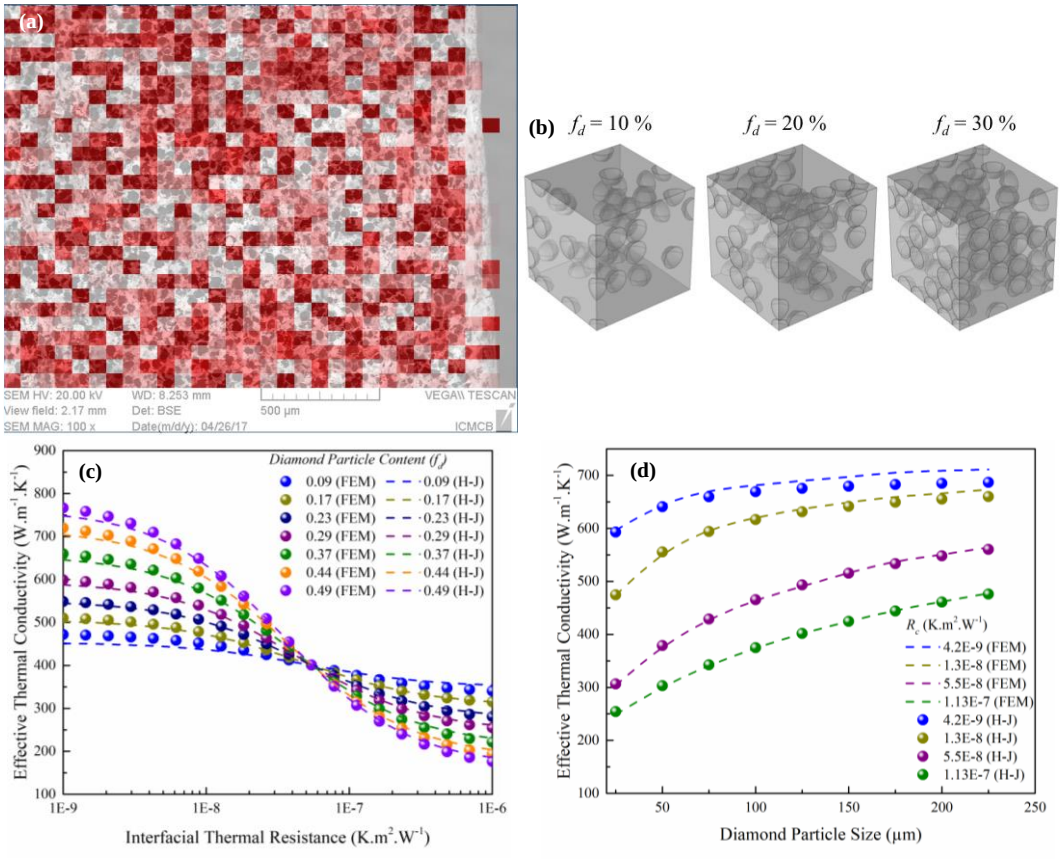

Figure 5: (a) Diamond particles distribution measured on a cross-section view by SEM at different volume fractions, (b) random normal distribution of diamond particles within the copper matrix used for finite element calculations of K_{eff} at different f_d. Calculated effective thermal conductivity as a function of (c) the thermal resistance R_c of the interface with f_d varying from 0.09 to 0.49, and (d) the particle diameter d with the interfacial thermal resistance R_c varying from 1×10^{-9} to 1×10^{-7} K.m^2.W^{-1} with f_d = 0.42. Spheres represent the realistic model and dashed lines represent the FE model.

The FE model has been used in order to retrieve the measured effective thermal conductivity for the Cu-D system. The value of the interfacial thermal resistance reported in **Figure 6(a)** that fits the experimental data, is $R_c = (1.62 \pm 0.15)\times10^{-7}$ m^2.K.W^{-1}. This value is obviously very high and consistent with the absence of chemical bonds, and very dissimilar phonon properties between diamond and copper. Also, the model tends to overestimate K_{eff} when $f_d >$ 0.4. That is due to an increasing porosity level with increasing diamond volume fraction (**Figure 6(b)**) which is a major drawback of powder metallurgy processes. As shown previously in **Figure 1(a)**, cross-sectional SEM analyses revealed that porosity occurs mainly at the Cu-D interface, leading to an even more important decrease of the interfacial conductance, and therefore a decrease of the effective thermal conductivity of the composite.

Porosity is not an issue in these composites, as the solid-liquid coexistent phase process allows full densification of high-volume fraction composites, thanks to the liquid phase which flows through the pores.

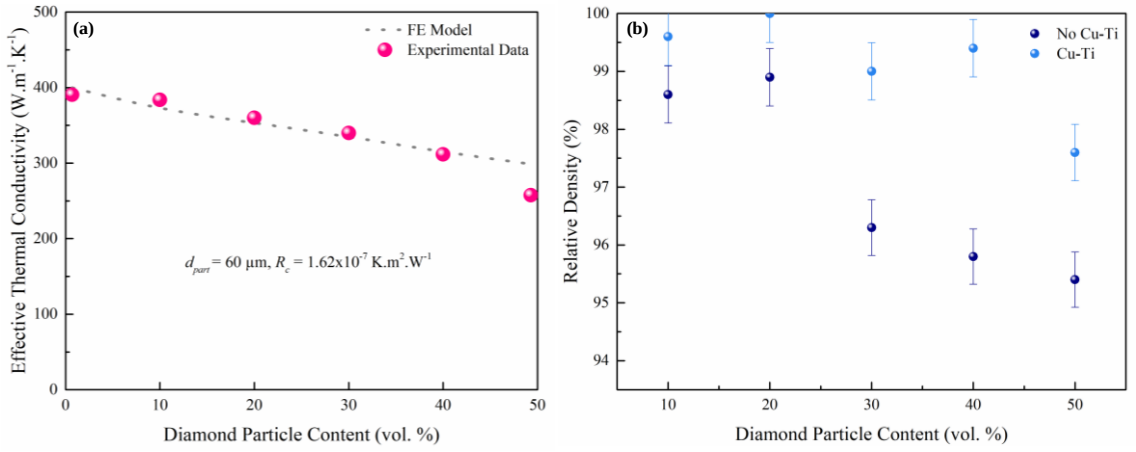

Figure 6: (a) Measured (pink spheres) and calculated (dashed line) thermal conductivities of Cu/D composite materials reinforced with diamond particles of d_{part} = 60 µm and an interfacial thermal resistance of (1.62 ± 0.15)×10^{-7} K.m^2.W^{-1}. (b) Relative density of composite materials with respect to the diamond volume fraction with and without Cu-Ti addition.

As presented in **Figure 7(a)**, the ratio $S(R_c)/S(k_d)$, with $S(x) = \partial K_{eff}/x\partial x$, of the two sensitivity functions on R_c and k_d according to f_d is not constant, proving thus that, both parameters R_c and k_d can be identified from the experimental data (knowing k_m). On the contrary, the ratio $S(R_c)/S(k_m)$ being constant, simultaneous identification of R_c and k_d is not feasible. Comparable conclusions are found, as shown in **Figure 7(b)**, regarding the variation of those two ratios according to d. As presented in **Figure 7(c)**, a good agreement between the experimental measurements and the simulated ones can be found when R_c = (1.12 ± 0.2)×10^{-8} K.m^2.W^{-1} and k_d = (1038 ± 80) W.m^{-1}.K^{-1} (we used the Levenberg-Marquardt minimization algorithm with 2×10^{-8} m^2.K.W^{-1} and 1500 W.m^{-1}.K^{-1} as initial values for R_c and k_d respectively). The comparison between theoretical data and measurements for the Cu(Cu-Ti)/D system is represented in **Figure 7(d)**. The remaining quantity of Ti within the Cu matrix, at the end of the sintering process, depends on the initial quantity inserted in the composite mixture. Indeed, large volume fractions of reinforcements, for the same Ti amount will lead to less Ti within the matrix. This trend can be observed for the composites containing 20, 30 and 40 vol.% of diamond particles and the fixed amount of 4 vol.% Cu-Ti alloy. The corresponding values of the metal matrix thermal conductivity is derived from the measurements of Lloyd et *al*[13]. We

found that the value R_c = (1.05 ± 0.2)×10^{-8} m^2.K.W^{-1} and k_d = (1040 ± 90) W.m^{-1}.K^{-1} allows the best fit for the experimental data, using the same procedure as previously. The identified value of k_d is consistent with the one we found for the Cu(Cu-Zr)/D system as well as the identified value of R_c for the Cu(Cu-Ti)/D system which is very close to that found for the Cu(Cu-Zr)/D system.

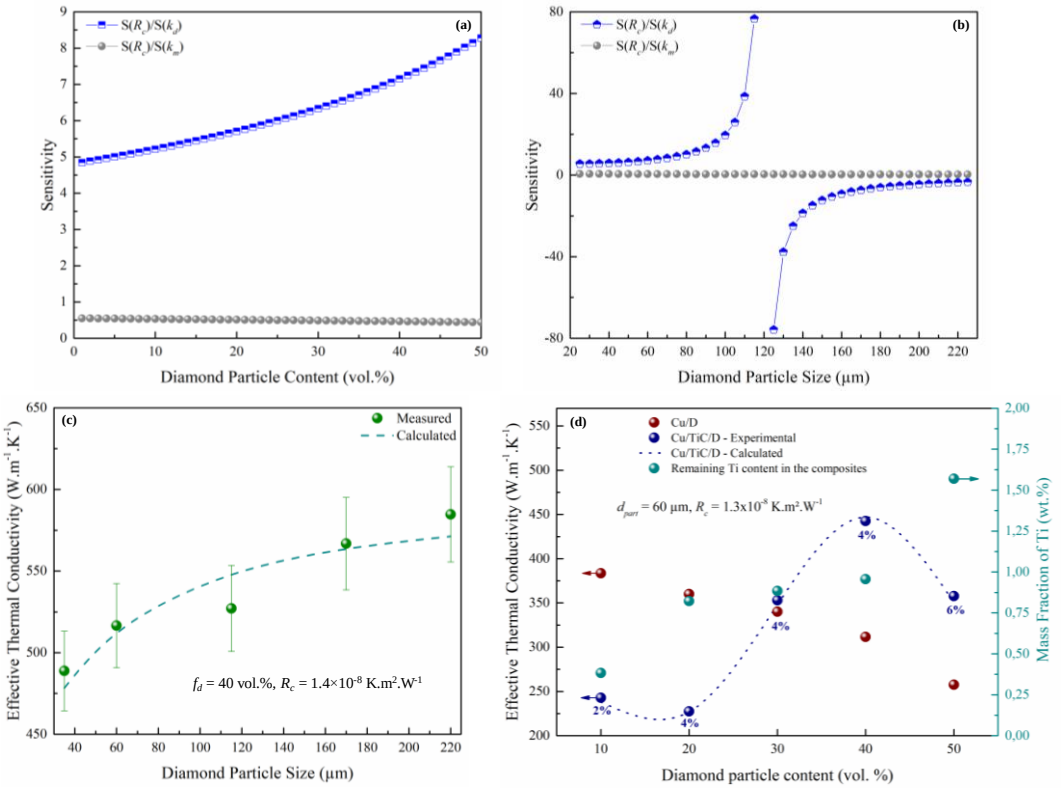

Figure 7: (a) ratio of the sensitivity functions of K_{eff} for {R_c and k_d} and for {R_c and k_m} according to f_d with k_m = 400 W.m^{-1}.K^{-1}, k_d = 1200 W.m^{-1}.K^{-1}, R_c = 10^{-7} K.m^2.W^{-1}, d = 60 µm. (b) ratio of the sensitivity functions of K_{eff} for {R_c and k_d} and for {R_c and k_m},according to d with k_m = 400 W.m^{-1}.K^{-1}, k_d = 1200 W.m^{-1}.K^{-1}, R_c = 10^{-7} K.m^2.W^{-1}, f_d = 0.4. Comparison of measured effective thermal conductivity of (c) the Cu(Cu-Zr)/D composite materials with the calculated values obtained using the H-J model from identified R_c and k_d parameters, and (d) the Cu(Cu-Ti)/D composite material with the calculated values (dashed line) obtained using the H-J model from identified R_c and k_d parameters. Initial Ti contents (vol.%) are indicated in blue for each value of f_d. Remaining contents (wt.%) of Ti within the composite materials are given by light blue spheres (right Y-axis).

3.3.Nanoscale analysis of interfacial thermal resistances

Phonon density of states *g(ω)* measurements from neutron scattering experiments for diamond, Cu, ZrC and TiC have been made by several authors and are reported in **Figure 8**. The phonon DOS for diamond has a prominent peak at 37 THz, thus very close to the cutoff frequency (about 40 THz), which results in optical modes associated to sp^3 bonds. The phonon DOS for Cu is located at about 7 THz, which is also the cutoff frequency. It is thus clear that the high difference in cutoff frequency for Cu and diamond limits the heat transfer through elastic phonon scattering, making therefore the inelastic scattering mandatory to enhance the thermal conductance of the interface. It was well demonstrated that anharmonic inelastic scattering (one diamond phonon splits into two equal frequency metal phonons) are mainly responsible for the conduction at the interface between diamond and Cu[17,32]. In addition, electron-phonon interactions within the metal, lead to a thermal resistance $R_{ep} = 1/\sqrt{Gk_{Cu,L}}$ in series with the phonon-phonon resistance, where $g = (5.73 \pm 0.15) \times 10^{16}\ W.m^{-3}.K^{-1}$ is the volume electron-phonon coupling factor in copper and $k_{Cu,L} = 8.45\ W.m^{-1}.K^{-1}$ is the lattice thermal conductivity of Cu. Using these values, this comes to $R_{ep} = (1.437 \pm 0.19) \times 10^{-9}\ K.m^2.W^{-1}$.

As reported by Liang and Tsai, using molecular dynamics (MD) simulations, inserting an interlayer whose Debye temperature is about the square root of the product of the Debye temperatures of the two solids, will enhance the thermal conductance between these two solids[33]. The optimal Debye temperature for an interfacial material between Cu and diamond should be $\Theta_{D,i,opt} = \sqrt{310 \times 1860} \approx 760\ K$. Therefore, TiC and ZrC could be potential candidates regarding this criterium, although the Debye temperature of TiC is closer to the optimal (**Table 2**).

Table 2: Density, thermal conductivity, specific heat, Debye temperature, longitudinal and transverse velocities, and melting temperature for Cu, TiC, ZrC, and diamond, found in the literature.

Material	Density ($kg.m^3$)	Thermal conductivity ($W.m^{-1}.K^{-1}$)	Specific heat capacity ($J.kg^{-1}.K^{-1}$)	Debye Temperature Θ_D (K)	v_T ; v_L (ms^{-1})	Melting point (K)	Cut-off frequency ω_c (THz)
Cu	8960	400	380	310	4760; 2300	1358	7

TiC	4910	21	190	614	1200; 6154	3067	18
ZrC	6590	20.5	205	491	9733; 5108	3420	20
Diamond	3520	1000-1500	630	1860	17600; 12800	3827	40

On the other hand, as shown in **Figure 8**, the phonon DOS for TiC and ZrC are very similar in terms of both spectral distribution and cutoff frequency, that is about 20 THz. As stated by English et *al*. and Shin et *al*., phonon DOS for materials located at both sides of an interface differs from bulk phonon DOS for each material. In fact, the presence of interfacial atomic restructuring is expected to reduce the phonon boundary resistance by providing additional transport channels [15,34].

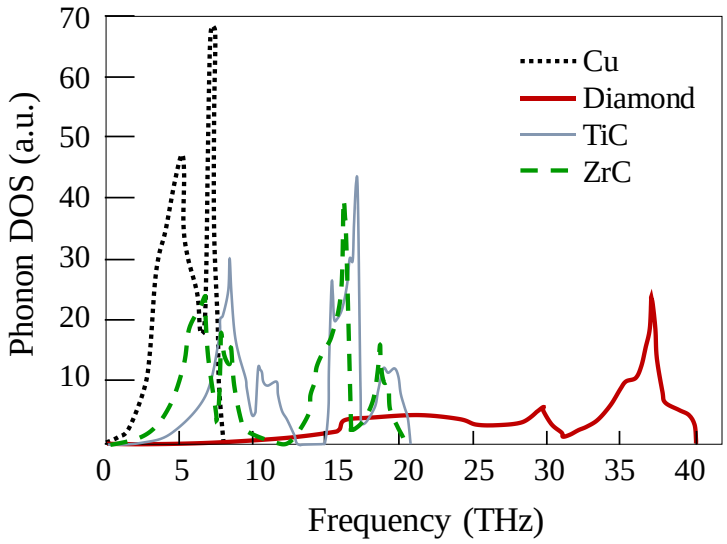

Figure 8: Phonon density of states g(ω) measured from neutron scattering experiments for diamond[35], Cu[36,37], ZrC[38], and TiC[39].

Therefore, the DOS spectra overlap spans a much larger range of frequencies than the one obtained from the bulk DOS. However, this change cannot be easily predicted in our configuration, therefore, the bulk DOS is used to calculate the theoretical thermal conductance. Hence, the obtained thermal conductance value must be viewed as the minimal one. On the other hand, all the simulations by MD presented in previous papers assumed Lennard-Jones (LJ) potentials, even within the case of a disordered interface. This cannot be

retained as a credible configuration in the present study since, as shown by Losego et *al.*[17], transition from van der Walls (Cu-diamond system) to covalent bonding (Cu-TiN and TiN-diamond systems) increases strongly the interfacial thermal conductance. The thermal boundary conductance was found to be most influenced by the interfacial chemical bonding as both the phonon flux and the vibrational mismatch between the materials are each subject to the interfacial bond strength. The phonon mean free path and thermal conductivity, k_i, of the interfacial material strongly influence the optimal thickness at which the interfacial thermal conductance h_c increases. The thermal resistance R_c of the interphase is therefore given by:

$$R_c = R_{Cu-i} + \frac{e_i}{k_i} + R_{i-D} \quad (2)$$

In this relation k_i is the thermal conductivity of the material which constitutes the interphase (TiC or ZrC), e_i is the thickness of the interphase, $R_{cu\text{-}i}$ is the thermal resistance of the interface between the interphase layer and copper and $R_{i\text{-}D}$ is the resistance of the interface between the interphase layer and the diamond. The thicknesses used in this calculation were e_{TiC} = 200 nm and e_{ZrC} = 125 nm. The interfacial resistance between two materials, *a* and *b*, is calculated using the asymptotic expression of the DMM at high temperature given by:

$$R_{a-b} = \frac{4}{\tau_{a-b} C_{p,a}(T) v_a}, \text{ with } \Theta_{D,a} < \Theta_{D,b} \quad (3)$$

where $\tau_{a\text{-}b}$ is the transmission coefficient of phonons at the interface between materials a and b, that is defined as $\tau_{a-b} = \sum_{j=1}^{3} v_{g,j,b}^{-2} / \left(\sum_{j=1}^{3} v_{g,j,b}^{-2} + \sum_{j=1}^{3} v_{g,j,a}^{-2}\right)$, with subscript *g* denoting either the transverse (T) or longitudinal (L) velocity, and v_a is the speed of sound in material a that is defined as $3/v_a^3 = 1/v_{L,a}^3 + 2/v_{T,a}^3$. Since the DMM assumes elastic phonon scattering (a phonon of frequency *w* will only transfer energy across an interface by scattering with another phonon of frequency *w*), it is relevant for the Cu/ZrC/D and Cu/TiC/D systems. For the Cu/D system, where scattering is mainly inelastic, the calculated resistance using the DMM has to be viewed only as qualitative. All the required properties for these calculations are reported in **Table 2**. Using this data, the values for τ and $R_{a\text{-}b}$ reported in **Table 3**, are calculated. Finally, the thermal resistance for the two interphases are: $R_{c,TiC}$ = (1.17 ± 0.15)×10^{-8} K.m^2.W^{-1} and $R_{c,ZrC}$ = (1.11 ± 0.14)×10^{-8} K.m^2.W^{-1}. It is not surprising to find that both interfacial materials lead to comparable values of thermal resistance. Also, one can notice that these values are reasonable for our composite materials; therefore, the thickness approximation made is acceptable. On the other hand, it is clear that the electronic contribution is one order of magnitude lower that that of phonons in R_c.

Table 3: Phonon transmission coefficients and thermal resistances of the interfaces involved in the studied systems.

Interface	τ	$R_{a\text{-}b}$ (K.m².W^{-1})
Cu-D	0.035	1.29×10^{-8}
Cu-TiC	0.124	3.67×10^{-9}
Cu-ZrC	0.171	2.65×10^{-9}
D-TiC	0.205	3.03×10^{-9}
D-ZrC	0.150	3.45×10^{-9}

4. Conclusions

In this work the effective thermal conductivities and heat transfers at the interphases of Cu(Cu-Ti)-D and Cu(Cu-Zr)-D systems were investigated. The composite materials were obtained using the solid-liquid coexistent phase process, which enhances the diffusion and reactivity of the carbide forming elements with the carbon reinforcements and allows full densification of composite materials with high contents of reinforcements. Cryofractures have confirmed the presence of a strong bonding between the Cu matrix and the diamond reinforcement by exhibiting the fragile rupture of the diamond reinforcements. The presence of ZrC interphases was shown to increase the thermal conductivities of the composite materials with respect to Cu/D composite materials with no interphases, which also confirms the strong bonding brought by the interphase. The highest thermal conductivities were obtained for the composite materials containing ZrC interphases rather than TiC, as Ti tends to drastically decrease the intrinsic thermal conductivity of the Cu matrix, even in very small concentrations. The effect of the diamond particle size was also discussed, and we confirmed that larger diamond particle sizes lead to higher effective thermal conductivities. The comparison of the simulations with the experimental results led to determine the thermal resistances of $R_{c,TiC} = (1.05 \pm 0.2)\times10^{-8}$ K.m^2.W^{-1} for the TiC interphases and $R_{c,ZrC} = (1.12 \pm 0.2)\times10^{-8}$ K.m^2.W^{-1} for the ZrC interphases. Finally, the heat transfer through the interphases was analyzed at the nanoscale. Thermal resistances at the interfaces between the metal-carbide interphase and carbide interphase-diamond were calculated using the Diffuse Mismatch Model. The values found for $R_{c,TiC}$ and $R_{c,ZrC}$ using this approach are very close to each other and are also very close to those extracted from bulk measurements.

Acknowledgement

The authors thank Mr. Eric Lebraud of the Institut de Chimie de la Matière Condensée de Bordeaux for performing the XRD analyses. This research did not receive any specific grant from funding agencies in the public, commercial, or not-for-profit sectors.

References

[1] T. Schubert, Ciupiński, W. Zieliński, A. Michalski, T. Weißgärber, and B. Kieback, Scr. Mater. **58**, 263 (2008).

[2] K. Yoshida and H. Morigami, Microelectron. Reliab. **44**, 303 (2004).

[3] J.-M. Tao, X.-K. Zhu, W.-W. Tian, P. Yang, and H. Yang, Trans. Nonferrous Met. Soc. China (English Ed. **24**, (2014).

[4] T. Schubert, B. Trindade, T. Weißgärber, and B. Kieback, Mater. Sci. Eng. A **475**, 39 (2008).

[5] W. Schmidt-Brücken, H.; Schlapp, Zeitschrift Für Angew. Phys. **32**, 307 (1971).

[6] B. Dewar, M. Nicholas, and P.M. Scott, J. Mater. Sci. **11**, 1083 (1976).

[7] Q. Kang, X. He, S. Ren, L. Zhang, M. Wu, C. Guo, W. Cui, and X. Qu, Appl. Therm. Eng. **60**, 423 (2013).

[8] K. Chu, Z. Liu, C. Jia, H. Chen, X. Liang, W. Gao, W. Tian, and H. Guo, J. Alloys Compd. **490**, 453 (2010).

[9] J. He, X. Wang, Y. Zhang, Y. Zhao, and H. Zhang, Compos. Part B Eng. **68**, 22 (2015).

[10] L. Weber and R. Tavangar, Scr. Mater. **57**, 988 (2007).

[11] Chung, Chih Yu, C.H. Chu, M.T. Lee, C.M. Lin, and S.J. Lin, Sci. World J. **2014**, (2014).

[12] J. Li, X. Wang, Y. Qiao, Y. Zhang, Z. He, and H. Zhang, Scr. Mater. **109**, 72 (2015).

[13] J.C. Lloyd, E. Neubauer, J. Barcena, and W.J. Clegg, Compos. Sci. Technol. **70**, 2284 (2010).

[14] H.T. Hall, Rev. Sci. Instrum. **31**, 125 (1960).

[15] T.S. English, J.C. Duda, J.L. Smoyer, D.A. Jordan, P.M. Norris, and L. V. Zhigilei, Phys. Rev. B - Condens. Matter Mater. Phys. **85**, (2012).

[16] T. Guillemet, J.M. Heintz, B. Mortaigne, Y. Lu, and J.F. Silvain, Adv. Eng. Mater. **20**, 1 (2018).

[17] M.D. Losego, M.E. Grady, N.R. Sottos, D.G. Cahill, and P. V. Braun, Nat. Mater. **11**, 502 (2012).

[18] J. Li, H. Zhang, L. Wang, Z. Che, Y. Zhang, J. Wang, M.J. Kim, and X. Wang, Compos. Part A Appl. Sci. Manuf. **91**, 189 (2016).

[19] J. Grzonka, J. Kruszewski, M. Rosi, Ł. Ciupi, A. Michalski, and K.J. Kurzyd, Mater. Charact. **99**, 188 (2015).

[20] Q.L. Che, J.J. Zhang, X.K. Chen, Y.Q. Ji, Y.W. Li, L.X. Wang, S.Z. Cao, L. Guo, Z. Wang, S.W. Wang, Z.K. Zhang, and Y.G. Jiang, Mater. Sci. Semicond. Process. **33**, 67 (2015).

[21] H. Bai, N. Ma, J. Lang, C. Zhu, and Y. Ma, Compos. Part B Eng. **52**, 182 (2013).

[22] A.M. Abyzov, M.J. Kruszewski, Ł. Ciupiński, M. Mazurkiewicz, A. Michalski, and K.J. Kurzydłowski, Mater. Des. **76**, 97 (2015).

[23] D.P.H. Hasselman and L.F. Johnson, J. Compos. Mater. **21**, 508 (1987).

[24] S. Whitaker, *The Method of Volume Averaging* (Springer Science & Business Media, 1999).

[25] C. Hsueh-Chia, AIChE J. **29**, 846 (2018).

[26] H.-C. CHANG, Chem. Eng. Commun. **15**, 83 (1982).

[27] C. Azina, J. Roger, A. Joulain, V. Mauchamp, B. Mortaigne, Y. Lu, and J.F. Silvain, J. Alloys Compd. **738**, 292 (2018).

[29] E. Ruffio, C. Pradere, A. Sommier, J.C. Batsale, A. Kusiak, and J.L. Battaglia, Int. J. Therm. Sci. (2018).

[30] H.E. Swanson, N.T. Gilfrich, and G.M. Ugrinic, U.S. Gov. Print. Off. Circ. Natl. Bur. Stand. 539 26 (1955).

[31] S. Nagarjuna, K. Balasubramanian, and D.S. Sarma, Mater. Sci. Eng. A **225**, 118 (1997).

[32] P.E. Hopkins, J.C. Duda, and P.M. Norris, J. Heat Transfer **133**, 062401 (2011).

[33] Z. Liang and H.L. Tsai, Int. J. Heat Mass Transf. **55**, 2999 (2012).

[34] S. Shin, M. Kaviany, T. Desai, and R. Bonner, Phys. Rev. B - Condens. Matter Mater. Phys. **82**, (2010).

[35] J.L. Warren, J.L. Yarnell, G. Dolling, and R.A. Cowley, Phys. Rev. **158**, 805 (1967).

[36] R.M. Nicklow, G. Gilat, H.G. Smith, L.J. Raubenheimer, and M.K. Wilkinson, Phys. Rev. **164**, 922 (1967).

[37] J. Prakash, B.S. Semwal, and P.K. Sharma, Acta Phys. Acad. Sci. Hungaricae **30**, 231 (1971).

[38] P.T. Jochym and K. Parlinski, Eur. Phys. J. B **15**, 265 (2000).

[39] L. Pintschovius, W. Reichardt, and B. Scheerer, J. Phys. C Solid State Phys. **11**, 1557 (1978).

[40] Z. Hashin, S. Shtrikman, J. Appl. Phys. **33**, 3125– 3131 (1962).

[41] Carson et *al*., International Journal of Heat and Mass Transfer **48**, 2150–2158 (2005).